Interval Quadratic Programming for Day-Ahead Dispatch of Uncertain Predicted Demand ⋆

Takayuki Ishizaki [a,g], Masakazu Koike [b,g], Nacim Ramdani [d,g], Yuzuru Ueda [c,g], Taisuke Masuta [e,g], Takashi Oozeki [f,g], Tomonori Sadamoto [a,g], and Jun-ichi Imura [a,g],

[a] *Tokyo Institute of Technology; 2-12-1, Ookayama, Meguro, Tokyo, 152-8552, Japan.*

[b] *Tokyo University of Marine Science and Technology; 4-5-7, Kounan, Minato, Tokyo, 108-0075, Japan.*

[c] *Tokyo University of Science; 6-3-1, Niijuku, Katsushika, Tokyo, 162-0825, Japan.*

[d] *Univ. Orléans, INSA-CVL, PRISME, EA 4229, F45072, Orléans, France.*

[e] *The Institue of Applied Energy; 14-2-1, Nishi-Shimbashi, Minato, Tokyo, 105-0003, Japan.*

[f] *National Institute of Advanced Industrial Science and Technology; 1-2-1, Namiki, Tsukuba, Ibaraki, 305-8564, Japan.*

[g] *CREST, Japan Science and Technology Agency; 4-1-8, Honcho, Kawaguchi, Saitama, 332-0012, Japan.*

Abstract

In this paper, we propose an interval quadratic programming method for the day-ahead scheduling of power generation and battery charge cycles, where the prediction uncertainty of power consumption and photovoltaic power generation is described as a parameter vector lying in an interval box. The interval quadratic programming is formulated as the problem of finding the tightest box, i.e., interval hull, that encloses the image of a function of the minimizer in parametric quadratic programming. To solve this problem in a computationally efficient manner, we take a novel approach based on a monotonicity analysis of the minimizer in the parametric quadratic programming. In particular, giving a tractable parameterization of the minimizer on the basis of the Karush-Kuhn-Tucker condition, we show that the monotonicity analysis with respect to the parameter vector can be relaxed to the sign pattern analysis of an oblique projection matrix. The monotonicity of the minimizer is found to be essential in the day-ahead dispatch problem, where uncertain predicted demand, described by a parameter vector, is dispatched to power generation and battery charge cycles while the economic cost is minimized. Finally, we verify the efficiency of the proposed method numerically, using experimental and predicted data for power consumption and photovoltaic power generation.

Key words: Interval Quadratic Programming, Monotonicity Analysis, Prediction Uncertainty, Demand Dispatch.

1 Introduction

Reductions in greenhouse gas emissions are recognized as a global goal, with renewable energy sources such as photovoltaic (PV) and wind power expected to contribute to an efficient solution. For example, large-scale penetration of PV power generators into Japanese houses is expected by 2030. In this situation, the total amount of PV power generation can cover approximately 50% of the peak power consumption, as well as 10% of the entire energy consumption [1].

With this background, we need to manage a power system that involves the traditional power generators as well as PV power generators and storage batteries while maintaining the balance among the amounts of power generation, demand, and battery charging power. To improve the economic efficiency of power system management, the day-ahead schedules of power generation and battery charge cycles can be based on day-ahead predictions of power consumption and PV power genera-

⋆ Corresponding author: T. Ishizaki, Tel. & Fax: +81-3-5734-2646.

Email addresses: `ishizaki@mei.titech.ac.jp` (Takayuki Ishizaki), `mkoike0@kaiyodai.ac.jp` (Masakazu Koike), `nacim.ramdani@univ-orleans.fr` (Nacim Ramdani), `ueda@ee.kagu.tus.ac.jp` (Yuzuru Ueda), `t-masuta@iae.or.jp` (Taisuke Masuta), `takashi.oozeki@aist.go.jp` (Takashi Oozeki), `sadamoto@cyb.mei.titech.ac.jp` (Tomonori Sadamoto), `imura@mei.titech.ac.jp` (Jun-ichi Imura).

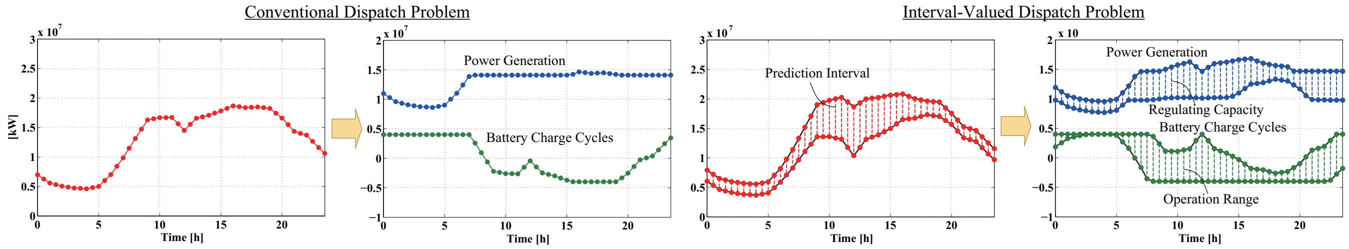

(a) Demand Prediction Profile

(b) Profiles of Power Generation and Battery Charge Cycles

(c) Demand Prediction Interval

(d) Intervals of Power Generation and Battery Charge Cycles

Fig. 1. Dispatch problems arising in scheduling of power generation and battery charge cycles.

tion [2–4]. In the following, we use the term "demand" to represent the defference between the total consumer demand and the amount of PV power generation. As shown in Figs. 1 (a) and (b), the minimization of economic cost, such as the fuel cost of generators and the deterioration of storage batteries, can be regarded as a dispatch problem in which the predicted demand profile is divided into that for power generation and for battery charge power.

However, sharp fluctuations in PV power generation and idiosyncratic power consumption make the exact prediction of demand profiles difficult. In view of this, a number of prediction methods for renewable energy generation have been developed in the literature. For example, [5] and [6] utilize weather forecasts and numerical simulations of meteorological phenomena to produce prediction profiles of renewable energy. On the other hand, as a relatively new approach, there are several methods for determining confidence intervals for renewable energy prediction [7,8], representing an interval in which prediction profiles are contained with a certain probability (e.g., 95%). To comply with such an interval-valued prediction method, we model the uncertain demand prediction as a set of all demand profiles that lie in an *interval box*. In particular, we use a confidence interval for PV power generation prediction produced by the method proposed in [9]. In this method, a prediction model based on support vector regression produces an interval with a predetermined confidence level from meteorological data [10], involving ambient temperature, humidity, and cloudiness. Its performance analysis is performed in [11] showing that the Laplacian distribution is better than the Gaussian distribution to approximate the expected variation of the prediction error coverage with relatively high confidence levels.

The day-ahead scheduling based on this type of prediction leads to an interval-valued dispatch problem, as shown in Figs. 1 (c) and (d). Note that our demand dispatch is clearly different from the standard one [3,12,13] in the sense that we deal with the prediction uncertainty as an interval-valued parameter. The resultant interval of power generation profiles corresponds to the regulating capacity of power generators that is sufficient to tolerate a given amount of prediction uncertainty.

In this paper, we perform the interval-valued dispatch via *interval quadratic programming*. The interval quadratic programming is formulated as the problem of finding the tightest box, i.e., interval hull, that encloses the image of an output function consisting of the minimizer of a parametric quadratic program, where the parameter vector lies in an interval box. The problem can also be regarded as a type of reachability analysis problems [14–16] in the context of parametric quadratic programming. This is because we aim at capturing the image of a mapping function defined over an interval box. It should be emphasized that such a problem is not necessarily easy to solve, because the exact interval hull is not obtained by calculating minimizers for a finite number of grid points in the parameter space.

To overcome this difficulty, we take a novel approach based on a monotonicity analysis to calculate the interval hull of interest. This novel approach has the advantage that we can calculate the exact interval hull in a finite number of operations. More specifically, it is theoretically guaranteed that the minimizer with respect to some extreme points of the interval box gives the exact interval hull. This approach has the potential to handle large-scale problems with high-dimensional decision variables and parameter space.

To clarify our theoretical contribution for interval-valued optimization, some references on interval analysis theory are in order. In fact, most studies on interval analysis focus on global optimization, i.e., finding the global extremum of a multi-modal multi-variable function [17,18], or on constraint satisfaction problems, i.e., covering a set of feasible solutions complying with equality and inequality constraints [19]. Towards these objectives, a constraint propagation technique is commonly used in conjunction with branch-and-bound algorithms [19,20]. Even though the application of these methods can address interval quadratic programming, this requires the direct computation and partition of the interval of real numbers, thereby incurring large computation loads. Moreover, overestimation often causes the resultant solution to be conservative.

Algorithms for parametric quadratic programming have been developed for model predictive control [21,22].

Even though these deal with a similar type of parametric quadratic programming, their focus is mainly on partitioning the parameter space with respect to the index sets of active inequality constraints. In this sense, their objective is clearly different from ours because we aim to capture the image of minimizers over the parameter space. Furthermore, the application of the algorithms in [21,22] to large-scale problems is not realistic, because their reliance on the iterative enhancement of the search space often entails a considerable computation load. To the best of our knowledge, there is no computationally efficient method to handle general interval-valued optimization. It should be noted that, even though the papers [23,24] handle nonlinear programming problems with interval-valued data, the problem formulation is totally different from that in this paper because they focus on calculating the optimal value bounds of an objective function.

In addition, we reference some related studies to clarify our contribution from the viewpoint of its application. Several studies on the scheduling of power generation and battery charge cycles have considered the prediction uncertainty using stochastic optimization [25–30] and fuzzy theory [31,32]. In these papers, power generation scheduling is performed to minimize the operational cost of generators from the viewpoint of worst-value and expected-value analyses. Note that their problem formulation is clearly different from ours, as we deal with the interval-valued dispatch problem on the basis of the interval prediction of renewable energy. In addition, even though interval optimization has been applied to environmental energy problems [33–35], the solution method involves the direct application of interval arithmetic, i.e., the extension of real algebraic operations to intervals, which can lead to conservative results due to overestimation.

Finally, we compare this paper with its preliminary versions [36,37], in which the scheduling of power generation and battery charge cycles is discussed on the premise of a single type of power generators. In this paper, we generalize the preliminary results to the case of multiple generator types, and explicitly consider the charge and discharge efficiency and the deterioration cost of storage batteries. This generalization makes our method more realistic in the sense that we can systematically deal with generators that have different specifications, such as time constants and fuel costs, while taking into account the energy loss due to the battery charge and discharge cycle. Note that, in this paper, we consider demand dispatch to multiple types of generators whereas we do not distinguish the same type of multiple generators as lumping them together. An allocation problem among an identical type of generators, corresponding to the current unit commitment [26,38], can be discussed after performing the uncertain demand dispatch here; see [39] for the day-ahead demand dispatch in the same perspective.

The remainder of this paper is structured as follows: In Section 2, we formulate the interval quadratic programming problem of finding the interval hull that encloses the image of a function of the minimizer in a parametric quadratic program. Then, in Section 3, we describe the day-ahead dispatch of uncertain demand to power generation and battery charge cycles using interval quadratic programming. Section 4 presents a solution to this problem on the basis of the notion of monotonicity. Then, in Section 5, we report the results of numerical experiments to verify the efficiency of our solution method. Finally, concluding remarks are provided in Section 6.

Notation. We denote the set of real numbers by $\mathbb{R}$, the set of nonnegative real numbers by $\mathbb{R}_{\geq 0}$, the n-dimensional unit matrix by I_n, the n-dimensional all-ones vector by $\mathbf{1}_n$, the all-ones matrix in $\mathbb{R}^{n\times m}$ by $\mathbf{1}_{n\times m}$, the ith column of I_n by e_i^n, the power set of a set M by $\mathfrak{P}(M)$, the cardinality of a set M by $|M|$, and the Kronecker product of matrices M_1 and M_2 by $M_1 \otimes M_2$. For a natural number n, let

$$\mathbb{N}[n] := \{1, \dots, n\}.$$

We denote a matrix composed of columns of I_n corresponding to the indices $\mathcal{I} \subseteq \mathbb{N}[n]$ by $e_{\mathcal{I}} \in \mathbb{R}^{n\times|\mathcal{I}|}$. Furthermore

$$E_{\mathcal{I}} := e_{\mathcal{I}} e_{\mathcal{I}}^{\mathsf{T}} \in \mathbb{R}^{n\times n}.$$

The block-diagonal matrix whose diagonal blocks are $M_1, \dots, M_n$ is denoted by $\mathrm{dg}(M_1, \dots, M_n)$, or simply $\mathrm{dg}(M_i)$ if there is no chance of confusion. For a function $f : \mathbb{R}^n \to \mathbb{R}^m$ and a closed domain $\mathcal{D} \subset \mathbb{R}^n$, the image of $f(\cdot)$ over $\mathcal{D}$ is denoted by

$$\mathrm{im}\, f(\mathcal{D}) := \{y \in \mathbb{R}^m : \exists d \in \mathcal{D} \ \text{ s.t. } \ y = f(d)\}.$$

Finally, a vector whose ith subvector is x_i is denoted by

$$[x_i]_{i\in\mathbb{N}[n]} := \left[\, x_1^{\mathsf{T}} \ \cdots \ x_n^{\mathsf{T}} \,\right]^{\mathsf{T}}.$$

2 Problem Formulation

We consider the following class of quadratic programming with a parameter vector $d \in \mathbb{R}^n$:

$$\mathtt{QP}(d) : \min_{x\in\mathbb{R}^\nu} \frac{1}{2} x^{\mathsf{T}} Q x - p^{\mathsf{T}} x \quad \text{s.t.} \ \begin{cases} A_{\mathrm{in}} x \ \leq \ b_{\mathrm{in}}(d) \\ A_{\mathrm{eq}} x \ = \ b_{\mathrm{eq}}(d) \end{cases} \tag{1}$$

where $Q = Q^{\mathsf{T}} \in \mathbb{R}^{\nu\times\nu}$ is assumed to be positive definite, $p \in \mathbb{R}^\nu$, $A_{\mathrm{in}} \in \mathbb{R}^{k_{\mathrm{in}}\times\nu}$, $A_{\mathrm{eq}} \in \mathbb{R}^{k_{\mathrm{eq}}\times N}$, $b_{\mathrm{in}} : \mathbb{R}^n \to \mathbb{R}^{k_{\mathrm{in}}}$, and $b_{\mathrm{eq}} : \mathbb{R}^n \to \mathbb{R}^{k_{\mathrm{eq}}}$. For a given d, let

$$x^*(d), \quad x^* : \mathbb{R}^n \to \mathbb{R}^\nu \tag{2}$$

denote the minimizer of $\mathtt{QP}(d)$ in (1). This minimizer can be found by an arbitrary algorithm for solving $\mathtt{QP}(d)$ with a fixed d. Furthermore, with regard to the minimizer, we define an output function $z^* : \mathbb{R}^n \to \mathbb{R}^m$ as

$$z^*(d) := Fx^*(d) + g(d) \tag{3}$$

where $F \in \mathbb{R}^{m\times\nu}$ and $g : \mathbb{R}^n \to \mathbb{R}^m$.

In the following, let us consider the parameter vector d to be uncertain and included in an interval box

$$[d] := [\underline{d}, \overline{d}] \subset \mathbb{R}^n \tag{4}$$

where $\underline{d}, \overline{d} \in \mathbb{R}^n$ correspond to the element-wise lower and upper limits of d. Taking a set-membership approach, we are interested in finding the element-wise lower and upper limits, i.e., interval hull, of the image $\mathcal{Z}^* := \mathrm{im}\, z^*([d])$ given by

$$[z^*] := [\underline{z}^*, \overline{z}^*] \subset \mathbb{R}^m, \quad \begin{cases} \underline{z}^* := \inf \mathcal{Z}^* \\ \overline{z}^* := \sup \mathcal{Z}^* \end{cases} \tag{5}$$

where the infimum and supremum are defined in the element-wise sense. Note that $[z^*]$ is the tightest box that encloses $\mathcal{Z}^*$. In this paper, we refer to the problem of finding this interval hull as *interval quadratic programming.*

Note that this problem is not necessarily easy to solve, because computing the values of $z^*(d)$ for a finite number of $d \in [d]$ does not generally give the interval hull $[z^*]$. One possible approach to compute the interval hull is the direct application of interval arithmetic, i.e., the extension of real algebraic operations to intervals. In practice, however, this approach leads to a conservative result, because the interval arithmetic encourages overestimation, and often suffers from a high computational load.

We overcome this difficulty by confining our attention to a specific class of problems. We devise an efficient interval quadratic programming solution via a monotonicity analysis, rather than using the interval arithmetic. Our approach is based on the fact that the lower and upper limits of the image of a monotonic function can be computed directly from the mapping of some extreme points of its argument, which is confined to an interval set.

3 Dispatch Problem of Uncertain Demand Via Interval Quadratic Programming

First, we introduce a mathematical model of the power system. Let $\mathbb{N}[n]$ be the time horizon of interest, and denote the power consumption and PV power generation at time t by p_t and p'_t, respectively. We denote the *net* demand at time t by

$$d_t := p_t - p'_t, \quad t \in \mathbb{N}[n]. \tag{6}$$

Furthermore, supposing that L generators are in operation, we denote the power generated by the lth generator at time t as $v_t^{(l)}$. With this notation, we model the temporal variation in the energy stored in the battery by

$$\begin{cases} y_{t+1} \;=\; y_t + \eta^{\mathrm{in}}\Delta y_t^{\mathrm{in}} - \dfrac{1}{\eta^{\mathrm{out}}}\Delta y_t^{\mathrm{out}} \\ \quad d_t \;=\; \displaystyle\sum_{l=1}^{L} v_t^{(l)} - (\Delta y_t^{\mathrm{in}} - \Delta y_t^{\mathrm{out}}), \end{cases} \quad t \in \mathbb{N}[n] \tag{7}$$

where $y_t \in \mathbb{R}$ denotes the battery stored energy, $\Delta y_t^{\mathrm{in}}, \Delta y_t^{\mathrm{out}} \in \mathbb{R}$ denote the battery charging and discharging power, and $\eta^{\mathrm{in}}, \eta^{\mathrm{out}} \in (0, 1]$ denote the constants representing the charge and discharge efficiency of the storage battery, respectively. Note that the initial battery energy y_1 is assumed to be a fixed constant. The second equality in (7) represents the balance among power generation, demand, and battery charge and discharge power.

Considering the physical limitation of the storage battery, we impose a set of inequality constraints on (7) as

$$\underline{y} \le y_t \le \overline{y}, \quad \begin{cases} 0 \le \Delta y_t^{\mathrm{in}} \le \overline{\Delta y}^{\mathrm{in}} \\ 0 \le \Delta y_t^{\mathrm{out}} \le \overline{\Delta y}^{\mathrm{out}}, \end{cases} \quad t \in \mathbb{N}[n] \tag{8}$$

where the underlined/overlined constants denote the lower/upper limits of the corresponding variables, representing the battery and inverter capacities. Furthermore, we impose an equality constraint on the battery stored energy as

$$y_{n+1} = y_1 \tag{9}$$

for the sustainable use of the storage battery. In the rest of this paper, we denote the variables to be determined as

$$\begin{aligned} v &:= [v^{(l)}]_{l\in\mathbb{N}[L]} \in \mathbb{R}^{Ln}, \\ y &:= [y_t]_{t\in\mathbb{N}[n]} \in \mathbb{R}^n, \quad \Delta y := \Delta y^{\mathrm{in}} - \Delta y^{\mathrm{out}} \in \mathbb{R}^n \end{aligned} \tag{10}$$

where $v^{(l)} := [v_t^{(l)}]_{t\in\mathbb{N}[n]}$, and the charge and discharge power profiles

$$\Delta y^{\mathrm{in}} := [\Delta y_t^{\mathrm{in}}]_{t\in\mathbb{N}[n]}, \quad \Delta y^{\mathrm{out}} := [\Delta y_t^{\mathrm{out}}]_{t\in\mathbb{N}[n]} \tag{11}$$

can be regarded as auxiliary variables. Note that Δy in (10) corresponds to the *net* battery charge and discharge power to be determined by optimization. In this notation, we define an objective function by

$$J(v, \Delta y^{\mathrm{out}}) := \sum_{t=1}^{n} \left\{ \sum_{l=1}^{L} f^{(l)}(v_t^{(l)}) + g(\Delta y_t^{\mathrm{out}}) \right\}, \quad (12)$$

where

$$f^{(l)}(x) := a_2^{(l)} x^2 + a_1^{(l)} x, \quad a_1^{(l)}, a_2^{(l)} \in \mathbb{R}_{\geq 0} \quad (13)$$

evaluates the fuel cost of the lth generator and

$$g(x) := b_2 x^2 + b_1 x, \quad b_1, b_2 \in \mathbb{R}_{\geq 0} \quad (14)$$

evaluates the battery deterioration cost caused by discharging. Their specifications will be given in Section 5.

In the following, let us regard d_t in (6) as a parameter vector that can vary within an interval. More specifically, given an interval box $[d]$ in (4), we consider the demand to be an uncertain predicted value lying in the interval box, namely

$$d := [d_t]_{t \in \mathbb{N}[n]} \in [d]. \quad (15)$$

Note that the interval box $[d]$ can be regarded as a confidence interval [7,8] of demand prediction. Let

$$\begin{aligned} & v^*(d), \quad v^* : \mathbb{R}^n \to \mathbb{R}^{Ln}, \\ & y^*(d), \quad y^* : \mathbb{R}^n \to \mathbb{R}^n, \quad \Delta y^*(d), \quad \Delta y^* : \mathbb{R}^n \to \mathbb{R}^n \end{aligned} \quad (16)$$

denote the minimizers of $J(v, \Delta y^{\mathrm{out}})$ in (12) subject to the inequality and equality constraints in (7), (8), and (9), which involve the interval parameter $d \in [d]$. In this notation, our objective is to find the interval hulls of $\mathrm{im}\, v^*([d])$, $\mathrm{im}\, y^*([d])$, and $\mathrm{im}\, \Delta y^*([d])$, denoted by

$$[v^*] := [\underline{v}^*, \overline{v}^*], \quad [y^*] := [\underline{y}^*, \overline{y}^*], \quad [\Delta y^*] := [\underline{\Delta y}^*, \overline{\Delta y}^*] \quad (17)$$

respectively, where the lower and upper limits are defined in the same manner as in (5).

Finally, let us rewrite the problem of finding the interval hulls in (17) using the interval quadratic programming in Section 2. Note that

$$\Delta y^{\mathrm{in}} = \Delta y^{\mathrm{out}} + \sum_{l=1}^{L} v^{(l)} - d \quad (18)$$

from the second equality in (7). Thus, we can eliminate the redundant variable as

$$x = \begin{bmatrix} x_1 \\ x_2 \end{bmatrix} \in \mathbb{R}^{(L+1)n}, \qquad \begin{cases} x_1 := v \in \mathbb{R}^{Ln} \\ x_2 := \Delta y^{\mathrm{out}} \in \mathbb{R}^n. \end{cases} \quad (19)$$

Using this elimination with the lower triangular matrix $M \in \mathbb{R}^{n \times n}$ whose (i,j)-element is given by

$$M_{i,j} = \begin{cases} 1, & i \geq j \\ 0, & i < j, \end{cases} \quad (20)$$

we obtain the parametric quadratic programming $\mathtt{QP}(d)$ in (1) where the coefficient matrices are given in (21). Furthermore, the output function

$$z^*(d) := \begin{bmatrix} v^*(d) \\ y^*(d) \\ \Delta y^*(d) \end{bmatrix}$$

can be rewritten in the form of (3) with

$$F := \begin{bmatrix} I_{Ln} & 0 \\ \mathbf{1}_L^{\mathsf{T}} \otimes M & 0 \\ \mathbf{1}_L^{\mathsf{T}} \otimes I_n & 0 \end{bmatrix}, \quad g(d) := -\begin{bmatrix} 0 \\ Md \\ d \end{bmatrix}. \quad (22)$$

Note that the size of the interval hull $[v^*]$ can be regarded as the minimal regulating capacity of power generators required to cover any demand prediction profile d lying in the confidence interval $[d]$. To reduce the redundant fuel cost of generators while maintaining a stable power supply, it is crucial to find the minimum regulating capacity sufficient to tolerate any possible demand prediction profile. Similarly, the sizes of $[y^*]$ and $[\Delta y^*]$ can be regarded as the required battery and inverter capacities with regard to the confidence interval of demand prediction.

4 Solution Method

4.1 Monotonicity-Based Approach

In this section, we analyse the parametric quadratic programming $\mathtt{QP}(d)$ in (1) from the viewpoint of monotonicity. To do this, we introduce the following definition:

Definition 1 Let an interval box $[d]$ in (4) be given. A function $f : \mathbb{R}^n \to \mathbb{R}^m$ is said to be *σ-monotone* if, for any $d \in [d]$, there exists $\sigma \in \{-1, 1\}^{m \times n}$ such that

$$\sigma_{i,j} \frac{\partial f_i(d)}{\partial d_j} \geq 0, \quad \forall i \in \mathbb{N}[m], \quad j \in \mathbb{N}[n] \quad (23)$$

where $\sigma_{i,j}$ denotes the (i,j)-element of σ, and $f_i(\cdot)$ and d_i denote the ith elements of $f(\cdot)$ and d, respectively.

The σ-monotonicity of $f(d)$ is defined as the existence of a sign matrix σ such that (23) holds, which means that

$$A_{\text{in}} := \begin{bmatrix} \mathbf{1}_L^\mathsf{T} \otimes I_n & I_n \\ -\mathbf{1}_L^\mathsf{T} \otimes I_n & -I_n \\ 0 & I_n \\ 0 & -I_n \\ \delta_1 \mathbf{1}_L^\mathsf{T} \otimes M & \delta_2 M \\ -\delta_1 \mathbf{1}_L^\mathsf{T} \otimes M & -\delta_2 M \end{bmatrix}, \quad b_{\text{in}}(d) := \begin{bmatrix} \overline{\Delta y}^{\text{in}} \mathbf{1}_n + d \\ -(\underline{\Delta y}^{\text{in}} \mathbf{1}_n + d) \\ \overline{\Delta y}^{\text{out}} \mathbf{1}_n \\ -\underline{\Delta y}^{\text{out}} \mathbf{1}_n \\ \overline{y} + \delta_1 M d \\ -(\underline{y} + \delta_1 M d) \end{bmatrix}, \quad A_{\text{eq}} := \begin{bmatrix} \delta_1 \mathbf{1}_L^\mathsf{T} \otimes \mathbf{1}_n^\mathsf{T} & \delta_2 \mathbf{1}_n^\mathsf{T} \end{bmatrix}, \quad b_{\text{eq}}(d) := \delta_1 \mathbf{1}_n^\mathsf{T} d$$

$$Q := \begin{bmatrix} \mathrm{dg}(\alpha_l^{-1}) \otimes I_n & 0 \\ 0 & I_n \end{bmatrix}, \quad p := -\frac{1}{2} \begin{bmatrix} \mathrm{dg}\left(\frac{a_1^{(l)}}{b_2} \right) \mathbf{1}_L \otimes \mathbf{1}_n & \frac{b_1}{b_2} \mathbf{1}_n \end{bmatrix}, \quad \alpha_l := \frac{b_2}{a_2^{(l)}}, \quad \delta_1 := \eta^{\text{in}}, \quad \delta_2 := \eta^{\text{in}} - \frac{1}{\eta^{\text{out}}} \tag{21}$$

the signs of $\partial f_i / \partial d_j$ are invariant with respect to $d \in [d]$. Note that, if $f(d)$ is σ-monotone, then we can obtain the lower and upper limits of the interval hull of $\mathrm{im}\, f([d])$ as

$$\underline{f} = [f_i(\underline{d}^{(i)})]_{i \in \mathbb{N}[m]}, \quad \overline{f} = [f_i(\overline{d}^{(i)})]_{i \in \mathbb{N}[m]} \tag{24}$$

where

$$\begin{aligned} \underline{d}^{(i)} &:= \left[\sigma_{i,j} \min \left\{ \sigma_{i,j} \underline{d}_j, \sigma_{i,j} \overline{d}_j \right\} \right]_{j \in \mathbb{N}[n]} \\ \overline{d}^{(i)} &:= \left[\sigma_{i,j} \max \left\{ \sigma_{i,j} \underline{d}_j, \sigma_{i,j} \overline{d}_j \right\} \right]_{j \in \mathbb{N}[n]} \end{aligned}$$

with $\underline{d}_j$ and $\overline{d}_j$ denoting the jth elements of $\underline{d}$ and $\overline{d}$. This implies that the element-wise infimum and supremum of the image are given by the mapping of some extreme points.

Next, we give a parameterization of $x^*(d)$ in (2) in terms of a family of index sets corresponding to active inequality constraints. From the Karush-Kuhn-Tucker (KKT) condition [40], we can state that, for the minimizer $x^*(d)$, there exist a nonnegative function $\lambda : \mathbb{R}^n \to \mathbb{R}^{6n}_{\geq 0}$ and a nonzero function $\mu : \mathbb{R}^n \to \mathbb{R} \backslash \{0\}$, called KKT multipliers, such that

$$\begin{cases} Q x^*(d) - p + A_{\text{in}}^\mathsf{T} \lambda(d) + A_{\text{eq}}^\mathsf{T} \mu(d) = 0 \\ \lambda^\mathsf{T}(d) \left[A_{\text{in}} x^*(d) - b_{\text{in}}(d) \right] = 0 \\ A_{\text{in}} x^*(d) - b_{\text{in}}(d) \leq 0 \\ A_{\text{eq}} x^*(d) - b_{\text{eq}}(d) = 0. \end{cases} \tag{25}$$

The KKT condition is generally a necessary condition for a local minimum, but it is sufficient for a global minimum if Q is positive definite. It is known that, for a fixed d, the set of indices corresponding to the positive elements of $\lambda(d)$ is compatible with the *active* inequality constraints against which the minimizer $x^*(d)$ collides. We refer to such an index set as the active index set. On the basis of this fact, we parameterize the minimizer as in the following lemma:

Lemma 1 Consider $\mathtt{QP}(d)$ in (1) with (21). Let $\mathcal{I} \in \mathfrak{P}(\mathbb{N}[6n])$ be such that

$$A_{\mathcal{I}} := \begin{bmatrix} e_{\mathcal{I}}^\mathsf{T} A_{\text{in}} \\ A_{\text{eq}} \end{bmatrix} \in \mathbb{R}^{(|\mathcal{I}|+1) \times (L+1)n} \tag{26}$$

is of full-row rank, and define

$$x^{\text{c}}(\mathcal{I}; d) = P_{\mathcal{I}} b_{\mathcal{I}}(d) + G_{\mathcal{I}} p \tag{27}$$

where

$$\begin{aligned} P_{\mathcal{I}} &:= Q^{-1} A_{\mathcal{I}}^\mathsf{T} (A_{\mathcal{I}} Q^{-1} A_{\mathcal{I}}^\mathsf{T})^{-1} \in \mathbb{R}^{(L+1)n \times |\mathcal{I}|} \\ G_{\mathcal{I}} &:= Q^{-1} - P_{\mathcal{I}} A_{\mathcal{I}} Q^{-1} \in \mathbb{R}^{(L+1)n \times (L+1)n} \end{aligned}$$

and

$$b_{\mathcal{I}}(d) := \begin{bmatrix} e_{\mathcal{I}}^\mathsf{T} b_{\text{in}}(d) \\ b_{\text{eq}}(d) \end{bmatrix}, \quad b_{\mathcal{I}} : \mathbb{R}^n \to \mathbb{R}^{|\mathcal{I}|+1}.$$

Then, for $x^*(d)$ in (2), it follows that

$$x^*(d) = x^{\text{c}}(\mathcal{I}^*(d); d) \tag{28}$$

where

$$\mathcal{I}^*(d) := \{ i \in \mathbb{N}[6n] : \lambda_i(d) > 0 \} \tag{29}$$

and $\lambda_i(d)$ denotes the ith element of $\lambda(d)$ in (25).

PROOF. If $\mathcal{I} = \mathcal{I}^*(d)$, it follows that

$$E_{\mathcal{I}} \lambda(d) = \lambda(d), \quad A_{\mathcal{I}} x^*(d) = b_{\mathcal{I}}(d).$$

Then, we have

$$x^*(d) = Q^{-1} p - Q^{-1} A_{\mathcal{I}}^\mathsf{T} \xi(d), \quad \xi(d) := \begin{bmatrix} e_{\mathcal{I}}^\mathsf{T} \lambda(d) \\ \mu(d) \end{bmatrix}. \tag{30}$$

Multiplying this by $A_{\mathcal{I}}$ from the left side, we have

$$b_{\mathcal{I}}(d) = A_{\mathcal{I}} Q^{-1} p - A_{\mathcal{I}} Q^{-1} A_{\mathcal{I}}^{\mathsf{T}} \xi(d),$$

where $A_{\mathcal{I}} Q^{-1} A_{\mathcal{I}}^{\mathsf{T}}$ is nonsingular owing to the full-row rankness of $A_{\mathcal{I}}$. Solving this equation with respect to $\xi(d)$ and substituting into (30), we obtain

$$x^*(d) = P_{\mathcal{I}} b_{\mathcal{I}}(d) + G_{\mathcal{I}} p. \tag{31}$$

This equation implies that (28) holds for (27) if $\mathcal{I} = \mathcal{I}^*(d)$. Hence, the claim follows. □

Lemma 1 parameterizes the minimizer $x^*(d)$ in (2) by $\mathcal{I} \in \mathfrak{P}(\mathbb{N}[6n])$, corresponding to the possible variation of active index sets. Note that, for a fixed $d \in [d]$, there exists a certain $\mathcal{I}^*(d)$ in (29) that represents the actual active index set. Using $x^{\mathrm{c}}(\mathcal{I}; d)$ in (27), it can readily be verified that $z^*(d)$ in (3) is σ-monotone if

$$z^{\mathrm{c}}(\mathcal{I}; d) := F x^{\mathrm{c}}(\mathcal{I}; d) + g(d)$$

is σ-monotone for all $\mathcal{I} \in \mathfrak{P}(\mathbb{N}[6n])$ such that $A_{\mathcal{I}}$ in (26) is of full-row rank.

4.2 Monotonicity Analysis

In this subsection, we show that σ-monotonicity is satisfied for $z^*(d)$ in (3) with (22). To this end, we first calculate the derivative of $x^{\mathrm{c}}(\mathcal{I}; d)$ in (27) as follows:

Lemma 2 Consider $\mathtt{QP}(d)$ in (1) with (21). For $\mathcal{I} \in \mathfrak{P}(\mathbb{N}[6n])$ such that $A_{\mathcal{I}}$ in (26) is of full-row rank, define

$$\mathcal{K}_i := \mathcal{K}_i^+ \cup \mathcal{K}_i^- \in \mathfrak{P}(\mathbb{N}[n]), \quad i \in \{1,2,3\} \tag{32}$$

where

$$\begin{cases} \mathcal{K}_i^+ := \{ j \in \mathbb{N}[n] : j + 2(i-1)n \in \mathcal{I} \} \\ \mathcal{K}_i^- := \{ j \in \mathbb{N}[n] : j + \{2(i-1)+1\}n \in \mathcal{I} \}. \end{cases}$$

Let k_i be the ith smallest element of $\tilde{\mathcal{K}}_3 := \mathcal{K}_3 \cup \{n\}$, and define

$$\mathcal{L}^{(i)} := \mathbb{N}[k_i] \backslash \mathcal{L}^{(i-1)}, \quad i \in \mathbb{N}[|\tilde{\mathcal{K}}_3|] \tag{33}$$

where $\mathcal{L}^{(0)}$ is regarded as the empty set. Then, it follows that

$$\frac{\partial x^{\mathrm{c}}(\mathcal{I}; d)}{\partial d} = Q^{-1} \Phi_{\mathcal{I}}^{\mathsf{T}} (\Phi_{\mathcal{I}} Q^{-1} \Phi_{\mathcal{I}}^{\mathsf{T}})^{-1} \Phi_{\mathcal{I}} \begin{bmatrix} I_n \\ 0 \end{bmatrix} \tag{34}$$

where $x^{\mathrm{c}}(\mathcal{I}; d)$ is defined as in (27) and

$$\begin{aligned} \Phi_{\mathcal{I}} &:= \begin{bmatrix} \mathbf{1}_L^{\mathsf{T}} \otimes e_{\mathcal{K}_1}^{\mathsf{T}} & e_{\mathcal{K}_1}^{\mathsf{T}} \\ 0 & e_{\mathcal{K}_2}^{\mathsf{T}} \\ \delta_1 \mathbf{1}_L^{\mathsf{T}} \otimes h^{\mathsf{T}} E_{\overline{\mathcal{K}}_1} & \delta_2 h^{\mathsf{T}} E_{\overline{\mathcal{K}}_1} \end{bmatrix} \\ h &:= \mathrm{dg}(\mathbf{1}_{|\mathcal{L}^{(i)}|}) \in \mathbb{R}^{n \times |\tilde{\mathcal{K}}_3|}, \quad \overline{\mathcal{K}}_1 := \mathbb{N}[n] \backslash \mathcal{K}_1. \end{aligned} \tag{35}$$

PROOF. By the fact that the first n columns of $A_{\mathcal{I}}$ coincide with $\partial b_{\mathcal{I}} / \partial d$, we notice that

$$\frac{\partial x^{\mathrm{c}}(\mathcal{I}; d)}{\partial d} = Q^{-1} A_{\mathcal{I}}^{\mathsf{T}} (A_{\mathcal{I}} Q^{-1} A_{\mathcal{I}}^{\mathsf{T}})^{-1} A_{\mathcal{I}} \begin{bmatrix} I_n \\ 0 \end{bmatrix}.$$

In the following, let us prove

$$Q^{-1} A_{\mathcal{I}}^{\mathsf{T}} (A_{\mathcal{I}} Q^{-1} A_{\mathcal{I}}^{\mathsf{T}})^{-1} A_{\mathcal{I}} = Q^{-1} \Phi_{\mathcal{I}}^{\mathsf{T}} (\Phi_{\mathcal{I}} Q^{-1} \Phi_{\mathcal{I}}^{\mathsf{T}})^{-1} \Phi_{\mathcal{I}}.$$

To this end, it suffices to show that

$$\mathrm{im}\ Q^{-1} A_{\mathcal{I}}^{\mathsf{T}} = \mathrm{im}\ Q^{-1} \Phi_{\mathcal{I}}^{\mathsf{T}}, \quad \ker A_{\mathcal{I}} = \ker \Phi_{\mathcal{I}}. \tag{36}$$

This is because (36) is equivalent to the existence of nonsingular matrices V and W such that

$$Q^{-1} A_{\mathcal{I}}^{\mathsf{T}} V = Q^{-1} \Phi_{\mathcal{I}}^{\mathsf{T}}, \quad W A_{\mathcal{I}} = \Phi_{\mathcal{I}}.$$

Note that $\mathcal{K}_i^+ \cap \mathcal{K}_i^- = \emptyset$ for all $i \in \{1,2,3\}$, because $A_{\mathcal{I}}$ in (26) is of full-row rank. This implies that $e_{\mathcal{I}}$ is given by

$$e_{\mathcal{I}}^{\mathsf{T}} = \begin{bmatrix} e_{\mathcal{K}_1^+}^{\mathsf{T}} & 0 & e_{\mathcal{K}_2^+}^{\mathsf{T}} & 0 & e_{\mathcal{K}_3^+}^{\mathsf{T}} & 0 \\ 0 & e_{\mathcal{K}_1^-}^{\mathsf{T}} & 0 & e_{\mathcal{K}_2^-}^{\mathsf{T}} & 0 & e_{\mathcal{K}_3^-}^{\mathsf{T}} \end{bmatrix},$$

which yields

$$A_{\mathcal{I}} = \mathrm{dg}(J_1, J_2, J_3, 1) \begin{bmatrix} \mathbf{1}_L^{\mathsf{T}} \otimes e_{\mathcal{K}_1}^{\mathsf{T}} & e_{\mathcal{K}_1}^{\mathsf{T}} \\ 0 & e_{\mathcal{K}_2}^{\mathsf{T}} \\ \delta_1 \mathbf{1}_L^{\mathsf{T}} \otimes e_{\mathcal{K}_3}^{\mathsf{T}} M & \delta_2 e_{\mathcal{K}_3}^{\mathsf{T}} M \\ \delta_1 \mathbf{1}_L^{\mathsf{T}} \otimes \mathbf{1}_n^{\mathsf{T}} & \delta_2 \mathbf{1}_n^{\mathsf{T}} \end{bmatrix}$$

where $J_i = \mathrm{dg}(I_{|\mathcal{K}_i^+|}, -I_{|\mathcal{K}_i^-|})$. Furthermore, because

$$\mathrm{im}\ h = \mathrm{im}\ M^{\mathsf{T}} e_{\tilde{\mathcal{K}}_3} = \mathrm{im} \begin{bmatrix} M^{\mathsf{T}} e_{\mathcal{K}_3} & \mathbf{1}_n \end{bmatrix}$$

by the definition of h and $\tilde{\mathcal{K}}_3$, and

$$\mathrm{im} \begin{bmatrix} e_{\mathcal{K}_1} & h \end{bmatrix} = \mathrm{im} \begin{bmatrix} e_{\mathcal{K}_1} & E_{\overline{\mathcal{K}}_1} h \end{bmatrix},$$

we verify the equality for the image in (36). The equality for the kernel is proven in the same manner. □

$$(\Phi_{\mathcal{I}} Q^{-1} \Phi_{\mathcal{I}}^{\mathsf{T}})^{-1} = \begin{bmatrix} (X - yz^{-1}y^{\mathsf{T}})^{-1} & -(X - yz^{-1}y^{\mathsf{T}})^{-1}yz^{-1} \\ \{-(X - yz^{-1}y^{\mathsf{T}})^{-1}yz^{-1}\}^{\mathsf{T}} & z^{-1} + z^{-1}y^{\mathsf{T}}(X - yz^{-1}y^{\mathsf{T}})^{-1}yz^{-1} \end{bmatrix} \tag{38}$$

Lemma 2 relaxes the monotonicity analysis of $x^{\mathrm{c}}(\mathcal{I}; d)$ to the sign analysis of the matrix in (34), which is composed of an oblique projection matrix. This representation makes the sign pattern analysis systematic as follows:

Lemma 3 In the same notation as that of Lemma 2, define

$$\Psi_{\mathcal{I}} := \alpha \begin{bmatrix} e_{\mathcal{K}_1} & 0 & \delta_1 E_{\overline{\mathcal{K}}_1} h \end{bmatrix} (\Phi_{\mathcal{I}} Q^{-1} \Phi_{\mathcal{I}}^{\mathsf{T}})^{-1} \Phi_{\mathcal{I}} \begin{bmatrix} I_n \\ 0 \end{bmatrix} \tag{37}$$

where $\alpha := \alpha_1 + \cdots + \alpha_L$. Then, for all $\mathcal{I} \in \mathfrak{P}(\mathbb{N}[6n])$ such that $A_{\mathcal{I}}$ in (26) is of full-row rank, all elements of $\Psi_{\mathcal{I}}$ are nonnegative and its diagonal elements are less than or equal to 1. In addition, for M defined as in (20), all elements of $M\Psi_{\mathcal{I}}$ are nonnegative and less than or equal to 1.

PROOF. From a direct calculation, we verify that

$$\Phi_{\mathcal{I}} Q^{-1} \Phi_{\mathcal{I}}^{\mathsf{T}} = \begin{bmatrix} X & y \\ y^{\mathsf{T}} & z \end{bmatrix}$$

where

$$\begin{aligned} X &:= \begin{bmatrix} (\alpha+1) I_{|\mathcal{K}_1|} & e_{\mathcal{K}_1}^{\mathsf{T}} e_{\mathcal{K}_2} \\ e_{\mathcal{K}_2}^{\mathsf{T}} e_{\mathcal{K}_1} & I_{|\mathcal{K}_2|} \end{bmatrix} \\ y &:= \begin{bmatrix} 0 \\ \delta_2 e_{\mathcal{K}_2}^{\mathsf{T}} E_{\overline{\mathcal{K}}_1} h \end{bmatrix}, \quad z := (\alpha \delta_1^2 + \delta_2^2) \mathrm{dg}(|\overline{\mathcal{K}}_1^{(i)}|) \end{aligned}$$

with $\overline{\mathcal{K}}_1^{(i)} := \overline{\mathcal{K}}_1 \cap \mathcal{L}^{(i)}$. Note that $\overline{\mathcal{K}}_1^{(i)} \neq \emptyset$ is guaranteed by the full-row rankness of $A_{\mathcal{I}}$. Thus, its blockwise inversion yields (38). Let $\mathcal{S}(X - yz^{-1}y^{\mathsf{T}})$ denote the Schur complement [41] of $X - yz^{-1}y$ with respect to $(\alpha+1)I_{|\mathcal{K}_1|}$. Furthermore, let $\mathcal{S}^{-1}(X - yz^{-1}y^{\mathsf{T}})$ denote its inverse. In the following, we evaluate the elements of $\Psi_{\mathcal{I}}$ by partitioning it as

$$\begin{aligned} \Theta_{11} &:= e_{\mathcal{K}_1}^{\mathsf{T}} \Psi_{\mathcal{I}} e_{\mathcal{K}_1}, \quad \Theta_{12} := e_{\mathcal{K}_1}^{\mathsf{T}} \Psi_{\mathcal{I}} e_{\overline{\mathcal{K}}_1} \\ \Theta_{21} &:= e_{\overline{\mathcal{K}}_1}^{\mathsf{T}} \Psi_{\mathcal{I}} e_{\mathcal{K}_1}, \quad \Theta_{22} := e_{\overline{\mathcal{K}}_1}^{\mathsf{T}} \Psi_{\mathcal{I}} e_{\overline{\mathcal{K}}_1}. \end{aligned} \tag{39}$$

Note that Θ_{11} and Θ_{22} correspond to the principal submatrices of $\Psi_{\mathcal{I}}$, and Θ_{12} and Θ_{21} correspond to its off-diagonal blocks. First, we notice that

$$\begin{aligned} \Theta_{11} &= \alpha \begin{bmatrix} I_{|\mathcal{K}_1|} & 0 \end{bmatrix} (\Phi_{\mathcal{I}} Q^{-1} \Phi_{\mathcal{I}}^{\mathsf{T}})^{-1} \begin{bmatrix} I_{|\mathcal{K}_1|} \\ 0 \end{bmatrix} \\ &= \alpha \begin{bmatrix} I_{|\mathcal{K}_1|} & 0 \end{bmatrix} (X - yz^{-1}y^{\mathsf{T}})^{-1} \begin{bmatrix} I_{|\mathcal{K}_1|} \\ 0 \end{bmatrix} \\ &= \alpha \mathcal{S}^{-1}(X - yz^{-1}y^{\mathsf{T}}). \end{aligned}$$

To evaluate this, let us denote the $(2,2)$-block of the Schur complement $\mathcal{S}(X - yz^{-1}y^{\mathsf{T}})$ by

$$\mathcal{S}_{22} := I_{|\mathcal{K}_2|} - \delta' e_{\mathcal{K}_2}^{\mathsf{T}} E_{\overline{\mathcal{K}}_1} \mathrm{dg}\left(\frac{1}{|\overline{\mathcal{K}}_1^{(i)}|} \mathbf{1}_{|\mathcal{L}^{(i)}| \times |\mathcal{L}^{(i)}|} \right) E_{\overline{\mathcal{K}}_1} e_{\mathcal{K}_2}$$

where $\delta' := \delta_2^2 / (\alpha\delta_1^2 + \delta_2^2)$. From $\mathcal{S}_{22} e_{\mathcal{K}_2}^{\mathsf{T}} e_{\mathcal{K}_1} = e_{\mathcal{K}_2}^{\mathsf{T}} e_{\mathcal{K}_1}$, it follows that $\mathcal{S}_{22}^{-1} e_{\mathcal{K}_2}^{\mathsf{T}} e_{\mathcal{K}_1} = e_{\mathcal{K}_2}^{\mathsf{T}} e_{\mathcal{K}_1}$. Thus, by the blockwise inversion of the Schur complement, we obtain

$$\begin{aligned} \Theta_{11} &= \alpha \left\{ (\alpha+1) I_{|\mathcal{K}_1|} - e_{\mathcal{K}_1}^{\mathsf{T}} e_{\mathcal{K}_2} \mathcal{S}_{22}^{-1} e_{\mathcal{K}_2}^{\mathsf{T}} e_{\mathcal{K}_1} \right\}^{-1} \\ &= \alpha \left\{ \alpha I_{|\mathcal{K}_1|} - e_{\mathcal{K}_1}^{\mathsf{T}} e_{\overline{\mathcal{K}}_2} e_{\overline{\mathcal{K}}_2}^{\mathsf{T}} e_{\mathcal{K}_1} \right\}^{-1} \\ &= I_{|\mathcal{K}_1|} - \frac{1}{\alpha+1} e_{\mathcal{K}_1}^{\mathsf{T}} e_{\overline{\mathcal{K}}_2} e_{\overline{\mathcal{K}}_2}^{\mathsf{T}} e_{\mathcal{K}_1} \end{aligned} \tag{40}$$

where $\overline{\mathcal{K}}_2 := \mathbb{N}[n] \backslash \mathcal{K}_2$. Hence, Θ_{11} is a diagonal matrix whose elements are all nonnegative and less than or equal to 1.

Next, we evaluate Θ_{22}. Let $\mathcal{K}_2^{(i)} := \mathcal{K}_2 \cap \mathcal{L}^{(i)}$. Because of

$$(X - yz^{-1}y^{\mathsf{T}})y = y\mathrm{dg}(\lambda_i)$$

where

$$\lambda_i := \frac{\alpha\delta_1^2 |\overline{\mathcal{K}}_1^{(i)}| + \left(|\overline{\mathcal{K}}_1^{(i)}| - |\overline{\mathcal{K}}_1^{(i)} \cap \mathcal{K}_2^{(i)}| \right) \delta_2^2}{(\alpha\delta_1^2 + \delta_2^2) |\overline{\mathcal{K}}_1^{(i)}|},$$

it follows that

$$Z := (X - yz^{-1}y^{\mathsf{T}})^{-1} y = y \mathrm{dg}(\lambda_i^{-1}). \tag{41}$$

Thus

$$\begin{aligned} \Theta_{22} &= \alpha \begin{bmatrix} 0 & \delta_1 e_{\overline{\mathcal{K}}_1}^{\mathsf{T}} h \end{bmatrix} (\Phi_{\mathcal{I}} Q^{-1} \Phi_{\mathcal{I}}^{\mathsf{T}})^{-1} \begin{bmatrix} 0 \\ \delta_1 h^{\mathsf{T}} e_{\overline{\mathcal{K}}_1} \end{bmatrix} \\ &= \alpha \delta_1^2 e_{\overline{\mathcal{K}}_1}^{\mathsf{T}} h (z^{-1} + z^{-1} y^{\mathsf{T}} Z z^{-1}) h^{\mathsf{T}} e_{\overline{\mathcal{K}}_1} \\ &= e_{\overline{\mathcal{K}}_1}^{\mathsf{T}} \mathrm{dg}\left(\mu_i \mathbf{1}_{|\mathcal{L}^{(i)}| \times |\mathcal{L}^{(i)}|} \right) e_{\overline{\mathcal{K}}_1} \\ &= \mathrm{dg}\left(\mu_i \mathbf{1}_{|\overline{\mathcal{K}}_1^{(i)}| \times |\overline{\mathcal{K}}_1^{(i)}|} \right) \end{aligned} \tag{42}$$

where

$$\mu_i := \frac{\alpha\delta_1^2}{\alpha\delta_1^2|\overline{\mathcal{K}}_1^{(i)}| + \left(|\overline{\mathcal{K}}_1^{(i)}| - |\overline{\mathcal{K}}_1^{(i)} \cap \mathcal{K}_2^{(i)}|\right)\delta_2^2} \tag{43}$$

are less than or equal to 1. Hence, all elements of Θ_{22} are nonnegative and less than or equal to 1. Furthermore, it follows from (41) that

$$\Theta_{12} = -\alpha \left[\, I_{|\mathcal{K}_1|} \ \ 0 \,\right] Z z^{-1} h^\top e_{\overline{\mathcal{K}}_1} = 0.$$

In the same manner, we can prove that $\Theta_{21} = 0$. Hence, it follows that all elements of $\Psi_{\mathcal{I}}$ are nonnegative and its diagonal elements are less than or equal to 1.

Finally, we prove that all elements of $M\Psi_{\mathcal{I}}$ are less than or equal to 1. Let M_i denote the ith row of M. Note that the element-wise inequality

$$0 \le M_i \le M_{i+1}$$

holds. The nonnegativity of the elements of $\Psi_{\mathcal{I}}$ implies $M_i\Psi_{\mathcal{I}} \le M_{i+1}\Psi_{\mathcal{I}}$. Thus, it suffices to show that all elements of

$$M_n\Psi_{\mathcal{I}} = \mathbf{1}_n^\top \Psi_{\mathcal{I}},$$

or equivalently $\mathbf{1}_{|\mathcal{K}_1|}^\top\Theta_{11}$ and $\mathbf{1}_{|\overline{\mathcal{K}}_1|}^\top\Theta_{22}$, are less than or equal to 1. From the diagonal structure of Θ_{11} in (40), we verify the claim for $\mathbf{1}_{|\mathcal{K}_1|}^\top\Theta_{11}$. On the other hand, from the block-diagonal structure of Θ_{22} in (42), we have

$$\mathbf{1}_{|\overline{\mathcal{K}}_1|}^\top\Theta_{22} = \mathbf{1}_{|\overline{\mathcal{K}}_1|}^\top \mathrm{dg}\left(\mu_i|\overline{\mathcal{K}}_1^{(i)}| I_{|\overline{\mathcal{K}}_1^{(i)}|}\right).$$

Note that $\mu_i|\overline{\mathcal{K}}_1^{(i)}| \le 1$ follows from the definition of μ_i in (43). Hence, the claim follows. □

We are now ready to state the main result of this paper. Lemma 3 leads to the following result on the σ-monotonicity of $z^*(d)$ in (3):

Theorem 4 Consider $\mathtt{QP}(d)$ in (1) with (21). Let

$$\sigma := \begin{bmatrix} \sigma^{(1)} \\ \sigma^{(2)} \\ \sigma^{(3)} \end{bmatrix} \in \{-1,1\}^{(L+2)n\times n} \tag{44}$$

where the (i,j)-element of $\sigma^{(1)} \in \{-1,1\}^{Ln\times n}$ is given as $\sigma_{i,j}^{(1)} = 1$, and those of $\sigma^{(2)}, \sigma^{(3)} \in \{-1,1\}^{n\times n}$ are given as

$$\sigma_{i,j}^{(2)} = \begin{cases} -1, & i \ge j \\ 1, & i < j, \end{cases} \qquad \sigma_{i,j}^{(3)} = \begin{cases} -1, & i = j \\ 1, & i \ne j, \end{cases} \tag{45}$$

respectively. Then, $z^*(d)$ in (3) with (22) is σ-monotone.

PROOF. Define $x_1^*(d)$ as the first subvector of $x^*(d)$ in (1) that is compatible with the partition in (19). To prove the claim, it suffices to show that $x_1^*(d)$ is $\sigma^{(1)}$-monotone and

$$(\mathbf{1}_L^\top \otimes M)x_1^*(d) - Md, \quad (\mathbf{1}_L^\top \otimes I_n)x_1^*(d) - d$$

are $\sigma^{(2)}$-monotone and $\sigma^{(3)}$-monotone, respectively.

Let us define $x_1^{\mathrm{c}}(\mathcal{I};d)$ as the first subvector of $x^{\mathrm{c}}(\mathcal{I};d)$ in (27). From (34) with (37), it follows that

$$\frac{\partial x_1^{\mathrm{c}}(\mathcal{I};d)}{\partial d} = \frac{1}{\alpha}\mathrm{dg}(\alpha_l)\mathbf{1}_L \otimes \Psi_{\mathcal{I}} \in \mathbb{R}_{\ge 0}^{Ln\times n}$$

for all $\mathcal{I} \in \mathfrak{P}(\mathbb{N}[6n])$ such that $A_{\mathcal{I}}$ in (26) is of full-row rank. Thus, $x_1^*(d)$ is $\sigma^{(1)}$-monotone. Furthermore, we have

$$\frac{\partial}{\partial d}\left\{(\mathbf{1}_L^\top \otimes I_n)x_1^{\mathrm{c}}(\mathcal{I};d) - d\right\} = \Psi_{\mathcal{I}} - I_n.$$

From Lemma 3, we notice that the sign pattern of $\Psi_{\mathcal{I}} - I_n$ is the same as $\sigma^{(3)}$, and that of $M(\Psi_{\mathcal{I}} - I_n)$ is the same as $\sigma^{(2)}$. Hence, the claim follows. □

Theorem 4 shows that $v^*(d)$, $y^*(d)$, and $\Delta y^*(d)$ in (16) are $\sigma^{(1)}$, $\sigma^{(2)}$, and $\sigma^{(3)}$-monotone, respectively. On the basis of this theorem, the interval hulls $[v^*]$, $[y^*]$, and $[\Delta y^*]$ in (17) are obtained as follows. First, $[v^*]$ is given by

$$\underline{v}^* = v^*(\underline{d}), \quad \overline{v}^* = v^*(\overline{d}),$$

which can be calculated by solving $\mathtt{QP}(d)$ in (1) with $\underline{d}$ and $\overline{d}$. In contrast, $[y^*]$ and $[\Delta y^*]$ are calculated in an element-wise manner. For example, the ith element of $\underline{y}^*$ is given by

$$\underline{y}_i^* = y_i^*(\underline{d}_y^{(i)}), \quad \underline{d}_y^{(i)} := \left[\, \underline{d}_1 \ \cdots \ \underline{d}_i \ \overline{d}_{i+1} \ \cdots \ \overline{d}_n \,\right]^\top$$

where $y_i^*(\cdot)$ denotes the ith element of $y^*(\cdot)$, and $\underline{d}_i$ and $\overline{d}_i$ denote the ith elements of $\underline{d}$ and $\overline{d}$. Note that $\underline{d}_y^{(i)}$ is not the same for all i. Thus, for $i \in \mathbb{N}[n]$, we find the minimizers of $\mathtt{QP}(d)$ with $\underline{d}_y^{(i)}$ to calculate the elements of $\underline{y}^*$. In this manner, we calculate $[y^*]$ and $[\Delta y^*]$. In conclusion, we can solve the interval quadratic programming in Section 2 with (21) and (22) by finding the minimizers of $\mathtt{QP}(d)$ with $4n + 2$ extreme points of the interval box $[d]$ in (4).

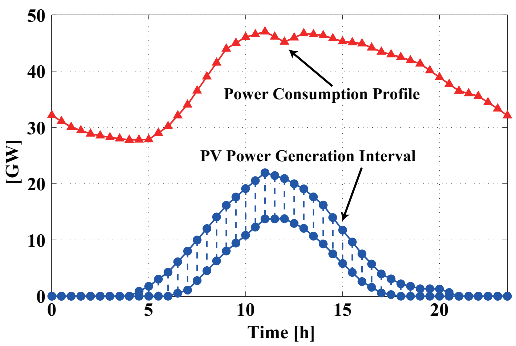

Fig. 2. Power consumption profile and confidence interval of PV power generation prediction.

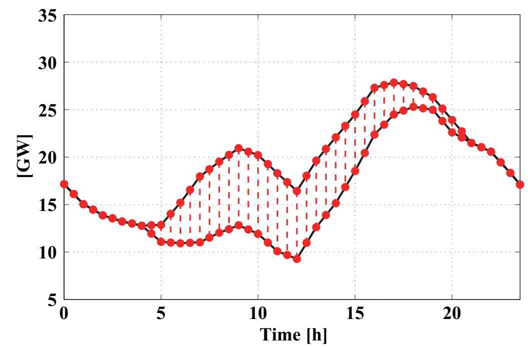

Fig. 3. Confidence interval of demand prediction.

5 Numerical Experiment

5.1 Parameter Settings

In this section, we examine the efficiency of the proposed method in solving the interval quadratic programming. We consider the scheduling of power generation and battery charge cycles in the Tokyo area, which has 19 million consumers. In the following, we suppose that five million consumers have PV power generators and three million have storage batteries, whose inverter and battery capacities average 3.3 kW and 33 kWh, respectively. These averages yield total capacities of 10 GW and 100 GWh. Furthermore, we suppose that three types of power generators are in operation and their operations are performed every 30 minutes, i.e., $L = 3$ and $n = 48$. Note that each type of power generators represents the total of several power generators with the same fuel cost.

The coefficients of $f^{(l)}(\cdot)$ in (13) are given as

$$\begin{aligned} a_1^{(1)} &= 2.0 \times 10^{-3}, \quad & a_2^{(1)} &= 2.0 \times 10^{-13}, \\ a_1^{(2)} &= 9.0 \times 10^{-4}, \quad & a_2^{(2)} &= 7.3 \times 10^{-13}, \\ a_1^{(3)} &= 2.2 \times 10^{-3}, \quad & a_2^{(3)} &= 2.5 \times 10^{-12}, \end{aligned}$$

which are determined so as to model the fuel cost functions in [1] by a quadratic function [42–45]. Furthermore, the coefficients of $g(\cdot)$ in (14) are given as

$$b_1 = 2.3\gamma \times 10^{-3}, \quad b_2 = 2.9\gamma \times 10^{-13} \tag{46}$$

where $\gamma \in [0, 1]$ is a weighting parameter described below. The values in (46) are determined in compliance with the price and durability of a standard lithium ion battery [46]. In this formulation, $\gamma = 1$ corresponds to the current cost and durability; thus, $\gamma < 1$ represents a future situation in which the deterioration cost has decreased.

Next, we construct a confidence interval for demand prediction, as in (15). For simplicity, let us suppose that the prediction of power consumption is exactly obtained as one profile, whereas that of PV power generation is obtained as a confidence interval. For the predicted power consumption profile, we use observation data from 18 June, 2010 [47], which is shown by the line with triangles in Fig. 2. The peak value of 43 GW is attained in the evening.The confidence interval of predicted PV power generation with the confidence level of 80% is given by the method in [9] with meteorological data from [10]. The extreme points of the intervals are shown by the lines with circles in Fig. 2. Note that the maximum difference between the extreme points is around 8.3 GW. By subtracting the predicted PV power generation intervals from the power consumption profile, we obtain the confidence interval of demand shown in Fig. 3. Note that 15 GW is subtracted in advance from the confidence interval; this is covered by basis generators such as nuclear plants.

5.2 Demand Dispatch to Power Generation and Battery Charge Cycles

On the basis of the confidence interval in Fig. 3, we schedule power generation and battery charge cycles by solving the interval quadratic programming. This clarifies the minimal required regulating capacities required by the generators, as well as those of the battery and inverter capacities. In this numerical experiment, we vary the weighting parameter γ in (46), reflecting the price of storage batteries, and the battery charge and discharge efficiencies η^{in} and η^{out} in (7).

First, with $\gamma = 1$ and $\eta^{\text{in}} = \eta^{\text{out}} = 0.9$, which correspond to the current price and the charge and discharge efficiencies of a standard battery, we calculate the interval hulls for power generation, battery charge cycles, and battery stored energy in the first, second, and third subfigures in Fig. 4 (a), respectively. In these subfigures, the lines with circles represent the extreme points of the interval hull for the corresponding variables. In this case, the use of storage batteries is not relatively significant, because their current quality is uneconomical in comparison with that of power generators. As a result, the

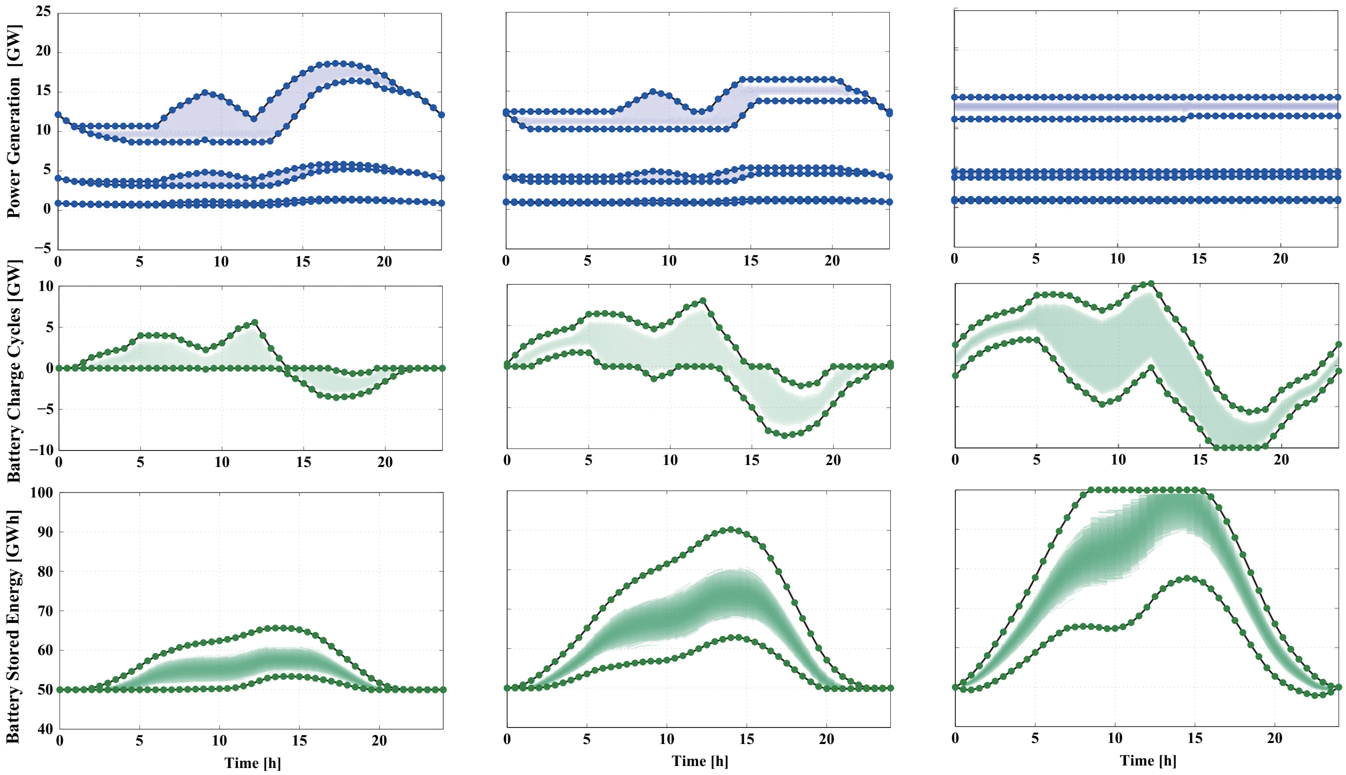

(a) Case 1: $\gamma = 1,\ \eta^{\text{in}} = \eta^{\text{out}} = 0.9$ **(b) Case 2:** $\gamma = 0,\ \eta^{\text{in}} = \eta^{\text{out}} = 0.9$ **(c) Case 3:** $\gamma = 0,\ \eta^{\text{in}} = \eta^{\text{out}} = 1$

Fig. 4. Interval hulls of power generation, battery charge and discharge cycles, and battery stored energy.

regulating capacities required by the generators are relatively large.

Next, with the same charge and discharge efficiency, we set $\gamma = 0$ to simulate the situation in which the price of storage batteries drops considerably. The results are shown in Fig. 4 (b). From this figure we can see that the use of storage batteries has increased compared with the situation in Fig. 4 (a). However, the maximal regulating capacities, i.e., the maximal size of power generation intervals, are comparable with those in Fig. 4 (a), even though the profiles corresponding to the power generation interval hull have become flatter.

Then, we set $\eta^{\text{in}} = \eta^{\text{out}} = 1$ and $\gamma = 0$ to simulate the ideal situation in which the use of storage batteries does not result in any economic loss. This extreme case analysis shows a possible limitation for regulation capacity reduction in a future situation where the price of batteries drops and their charge and discharge efficiencies are improved. The results are shown in Fig. 4 (c). From this figure, we can see that the use of storage batteries is maximized within the limits of the inverter and battery capacities. Owing to this, the required regulating capacity is reduced, and the profile corresponding to the power generation interval hull become almost flat.

Finally, we show the efficiency of our method in comparison with a brute-force approach. To this end, we randomly sample 10,000 demand prediction profiles from the confidence interval, and then calculate the corresponding optimal power generation, battery charge cycles, and battery stored energy profiles. In Figs. 4 (a)–(c), the colour distribution between the profiles of the interval hulls reflects the number of profiles passing through the corresponding point. From these results, we can see that the optimal power generation and battery charge cycle profiles are almost uniformly distributed in the interval hulls, whereas those of battery stored energy are non-uniformly distributed. This implies that even 10,000 samples, considerably more than the $4n + 2 = 194$ extreme points needed to calculate all interval hulls, cannot properly capture the limits of the optimal profiles.

6 Concluding Remarks

In this paper, we have proposed a solution method for a class of interval quadratic programming. Our approach is compatible with the problem of dispatching uncertain predicted demand to power generation and battery charge cycles. The interval quadratic programming was formulated as the problem of finding the interval hull that tightly encloses the image of an output function consisting of the minimizer in a parametric quadratic program. To solve this problem efficiently, we developed a novel approach based on a monotonicity analysis of this minimizer. Furthermore, we clarified that the minimizer in the dispatch problem of uncertain predicted demand possesses the monotonicity property. This allowed us to numerically verify the efficiency of the proposed method using experimental and predicted data for power consumption and PV power generation.

The validity of our approach for the interval quadratic programming is reliant on the monotonicity property of minimizers in the parametric quadratic program of interest. In view of this, the extension of our theory to more general dispatch problems is not necessarily straightforward. More specifically, it is not trivial to show whether the monotonicity property of these minimizers is inherent in more complicated dispatch problems, such as those involving the limitations on the amount of power generation and the suppression of PV power generation. One possible way to handle such a complicated problem is to partition the parameter space into several regions, each of which contains a locally monotonic minimizer. The development of such a method based on parameter space partitioning will be pursued in future work.

References

[1] T. Masuta, A. Yokoyama, Supplementary load frequency control by use of a number of both electric vehicles and heat pump water heaters, Smart Grid, IEEE Transactions on 3 (3) (2012) 1253–1262.

[2] R. Hanna, J. Kleissl, A. Nottrott, M. Ferry, Energy dispatch schedule optimization for demand charge reduction using a photovoltaic-battery storage system with solar forecasting, Solar Energy 103 (2014) 269–287.

[3] Y. Riffonneau, S. Bacha, F. Barruel, S. Ploix, Optimal power flow management for grid connected pv systems with batteries, Sustainable Energy, IEEE Transactions on 2 (3) (2011) 309–320.

[4] L. Li, Q. Ding, H. Li, M. Dan, Optimal dispatching method for smoothing power fluctuations of the wind-photovoltaic-battery hybrid generation system, in: Innovative Smart Grid Technologies Asia (ISGT Asia), 2012 Proceedings of the IEEE, IEEE, 2012, pp. 1–6.

[5] S. Bofinger, G. Heilscher, Solar electricity forecast-approaches and first results, in: European Photovoltaic Solar Energy Conference (EU PVSEC), 2006, no. 9, 2006, pp. 4–8.

[6] K. W. Appel, R. C. Gilliam, N. Davis, A. Zubrow, S. C. Howard, Overview of the atmospheric model evaluation tool (amet) v1. 1 for evaluating meteorological and air quality models, Environmental Modelling & Software 26 (4) (2011) 434–443.

[7] B. Petiau, Confidence interval estimation for short-term load forecasting, in: PowerTech, 2009 IEEE Bucharest, IEEE, 2009, pp. 1–6.

[8] A. Seppälä, Load research and load estimation in electricity distribution, Technical Research Centre of Finland, 1996.

[9] J. G. Silva Fonseca, T. Oozeki, H. Ohtake, K. Ogimoto, Preliminary study on prediction intervals for regional forecasts of photovoltaic power generation in Japan.

[10] Japan Meteorological Business Support Center (JMBSC). Available at: `http://www.jmbsc.or.jp/`.

[11] J. G. Silva Fonseca, T. Oozeki, H. Ohtake, K.-i. Shimose, T. Takashima, K. Ogimoto, Development of a method to provide prediction intervals for forecasts of power generation of photovoltaic systems.

[12] J.-H. Teng, S.-W. Luan, D.-J. Lee, Y.-Q. Huang, Optimal charging/discharging scheduling of battery storage systems for distribution systems interconnected with sizeable pv generation systems, Power Systems, IEEE Transactions on 28 (2) (2013) 1425–1433.

[13] M. Dicorato, G. Forte, M. Pisani, M. Trovato, Planning and operating combined wind-storage system in electricity market, Sustainable Energy, IEEE Transactions on 3 (2) (2012) 209–217.

[14] N. Ramdani, N. Meslem, Y. Candau, A hybrid bounding method for computing an over-approximation for the reachable set of uncertain nonlinear systems, Automatic Control, IEEE Transactions on 54 (10) (2009) 2352–2364.

[15] M. Althoff, Reachability analysis and its application to the safety assessment of autonomous cars, Technische Universitt Mnchen.

[16] C. Le Guernic, A. Girard, Reachability analysis of linear systems using support functions, Nonlinear Analysis: Hybrid Systems 4 (2) (2010) 250–262.

[17] K. Ichida, Constrained optimization using interval analysis, Computers & industrial engineering 31 (3) (1996) 933–937.

[18] I. Mazhoud, K. Hadj-Hamou, J. Bigeon, G. Remy, Interval-based global optimization in engineering using model reformulation and constraint propagation, Engineering Applications of Artificial Intelligence 25 (2) (2012) 404–417.

[19] L. Jaulin, Applied interval analysis: with examples in parameter and state estimation, robust control and robotics, Springer, 2001.

[20] E. Hansen, G. W. Walster, Global optimization using interval analysis: revised and expanded, Vol. 264, CRC Press, 2003.

[21] A. Bemporad, M. Morari, V. Dua, E. N. Pistikopoulos, The explicit linear quadratic regulator for constrained systems, Automatica 38 (1) (2002) 3–20.

[22] P. TøNdel, T. A. Johansen, A. Bemporad, An algorithm for multi-parametric quadratic programming and explicit mpc solutions, Automatica 39 (3) (2003) 489–497.

[23] W. Li, X. Tian, Numerical solution method for general interval quadratic programming, Applied mathematics and computation 202 (2) (2008) 589–595.

[24] M. Hladík, Optimal value bounds in nonlinear programming with interval data, Top 19 (1) (2011) 93–106.

[25] A. Sturt, G. Strbac, Efficient stochastic scheduling for simulation of wind-integrated power systems, Power Systems, IEEE Transactions on 27 (1) (2012) 323–334.

[26] S. Bu, F. R. Yu, P. X. Liu, Stochastic unit commitment in smart grid communications, in: Computer Communications Workshops (INFOCOM WKSHPS), 2011 IEEE Conference on, IEEE, 2011, pp. 307–312.

[27] P. Arun, R. Banerjee, S. Bandyopadhyay, Optimum sizing of photovoltaic battery systems incorporating uncertainty through design space approach, Solar Energy 83 (7) (2009) 1013–1025.

[28] N. Yang, C. Yu, F. Wen, C. Chung, An investigation of reactive power planning based on chance constrained programming, International Journal of Electrical Power & Energy Systems 29 (9) (2007) 650–656.

[29] C. Abbey, G. Joós, A stochastic optimization approach to rating of energy storage systems in wind-diesel isolated grids, Power Systems, IEEE Transactions on 24 (1) (2009) 418–426.

[30] R. Aihara, A. Yokoyama, F. Nomiyama, N. Kosugi, Impact of operational scheduling of pumped storage power plant considering excess energy and reduction of fuel cost on power supply reliability in a power system with a large penetration of photovoltaic generations, in: Power System Technology (POWERCON), 2010 International Conference on, IEEE, 2010, pp. 1–6.

[31] M. Suman, M. Venu Gopala Rao, G. Naga Kumar, O. Chandra Sekhar, Load frequency control of three unit interconnected multimachine power system with pi and fuzzy controllers, in: Advances in Electrical Engineering (ICAEE), 2014 International Conference on, IEEE, 2014, pp. 1–5.

[32] R.-H. Liang, J.-H. Liao, A fuzzy-optimization approach for generation scheduling with wind and solar energy systems, Power Systems, IEEE Transactions on 22 (4) (2007) 1665–1674.

[33] Q. Lin, G. Huang, IPEM: an interval-parameter energy systems planning model, Energy Sources, Part A 30 (14-15) (2008) 1382–1399.

[34] Y. Zhu, Y. Li, G. Huang, Planning municipal-scale energy systems under functional interval uncertainties, Renewable Energy 39 (1) (2012) 71–84.

[35] L. He, G. H. Huang, G. Zeng, H. Lu, An interval mixed-integer semi-infinite programming method for municipal solid waste management, Journal of the Air & Waste Management Association 59 (2) (2009) 236–246.

[36] M. Koike, T. Ishizaki, Y. Ueda, T. Masuta, T. Oozeki, N. Ramdani, T. Sadamoto, J.-i. Imura, Planning of optimal daily power generation tolerating prediction uncertainty of demand and photovoltaics (2014) 3657–3662.

[37] T. Ishizaki, M. Koike, N. Ramdani, J.-i. Imura, Monotonicity characterization of interval quadratic programming, in: Proceedings of the 21st International Symposium on Mathematical Theory of Networks and Systems, 2014, pp. 792–799.

[38] I. G. Damousis, A. G. Bakirtzis, P. S. Dokopoulos, A solution to the unit-commitment problem using integer-coded genetic algorithm, Power Systems, IEEE Transactions on 19 (2) (2004) 1165–1172.

[39] T. Sadamoto, T. Ishizaki, M. Koike, Y. Ueda, J.-i. Imura, Spatiotemporally multiresolutional optimization toward supply-demand-storage balancing under pv prediction uncertainty, Smart Grid, IEEE Transactions on 6 (2) (2015) 853–865.

[40] M. S. Bazaraa, H. D. Sherali, C. M. Shetty, Nonlinear programming: theory and algorithms, John Wiley & Sons, 2013.

[41] D. S. Bernstein, Matrix mathematics: theory, facts, and formulas, Princeton University Press, 2009.

[42] G. F. Reid, L. Hasdorff, Economic dispatch using quadratic programming, Power Apparatus and Systems, IEEE Transactions on 92 (6) (1973) 2015–2023.

[43] Z. Qiu, G. Deconinck, R. Belmans, A literature survey of optimal power flow problems in the electricity market context, in: Power Systems Conference and Exposition (PSCE), 2009 IEEE/PES, IEEE, 2009, pp. 1–6.

[44] A. J. Wood, B. F. Wollenberg, Power generation, operation, and control, John Wiley & Sons, 2012.

[45] R. Bhattacharya, C. K. Panigrahi, Dynamic economic load dispatch using classical and soft computing techniques, in: Green Computing Communication and Electrical Engineering (ICGCCEE), 2014 International Conference on, IEEE, 2014, pp. 1–6.

[46] Specification of lithium ion batteries. `http://www.edisonpower.co.jp/_file/epups-ver14.pdf`.

[47] Tokyo Electric Power Co. Available at: http://www.tepco.co.jp/forecast/.